

Phase-Inversion Waves in Oscillators Coupled by Two Kinds of Inductors as a Ladder

Masayuki YAMAUCHI^{†a)}, Yoshifumi NISHIO^{††}, Members, Akio USHIDA^{†††}, Fellow, and Mamoru TANAKA[†], Member

SUMMARY In this study, nonlinear wave phenomena related to transmissions and reflections of the phase-inversion waves around a discontinuity of a coupled system consisting of two kinds of arrays of van der Pol oscillators are investigated. By computer simulations, behavior of the phase-inversion waves around the discontinuity in the coupled system is classified into eight types. Further, the mechanisms of the transmission and the reflection of a phase-inversion wave at the discontinuity are explained. Circuit experiments confirm the simulated results.

key words: coupled oscillators, synchronization, wave propagation, phase difference, phase-inversion wave

1. Introduction

Large number of coupled limit-cycle oscillators are useful as models for a wide variety of systems in natural fields, for example, diverse physiological organs including gastrointestinal tracts and axial fiber of nervous systems, convecting fluids, arrays of Josephson junctions and so on. Hence, it is very important to analyze synchronization and the related phenomena observed in coupled oscillators in order to clarify mechanisms of generations or in order to control the generating-conditions of various phenomena in such natural systems [1]–[4]. In the field of the electrical engineering, a lot of studies on synchronization phenomena of coupled van der Pol oscillators have been carried out up to now [5]–[12]. Recently, we have discovered very interesting wave propagation phenomena of phase states between two adjacent van der Pol oscillators coupled by inductors as a ladder [13]. In the study, we named the continuously existing wave of changing phase states between two adjacent oscillators from in-phase to anti-phase or from anti-phase to in-phase as “phase-inversion wave.” Further, we reported the detail on “phase-wave” in [14], which is propagation of the phase difference less than 180 degrees between two adjacent oscillators. The phase-waves exist only in the transient states

unlike the phase-inversion waves. When the phase difference of a phase-wave is smaller than angle drawn into the anti-phase, the phase-wave disappears. Phase difference decreases as the phase-wave propagates. When the phase difference of a phase-wave is larger than angle drawn into the anti-phase, the phase-wave changes to the phase-inversion wave. Phase difference increases as the phase-wave propagates [5], [14]. Thus, the phase-waves change to phase-inversion waves or disappear.

In this study, by computer simulations, we observe behavior of the phase-inversion waves around a discontinuity in a coupled system consisting of two kinds of arrays of van der Pol oscillators and classify the phenomena. We explain the mechanisms of the transmission and the reflection of the phase-inversion waves at the discontinuity by using the relationship between phase difference and instantaneous frequency. We also carry out circuit experiments.

2. Circuit Model

Circuit model is shown in Fig. 1. In the circuit, N_2 identical van der Pol oscillators are coupled as an array by inductors. From the 1st to the N_1 th oscillators they are coupled by inductors L_{00} , while from the N_1 th to the N_2 th oscillators they are coupled by L_{01} . Consequently, there is a discontinuity at the N_1 th oscillator.

At first, the $v-i$ characteristics of the nonlinear negative resistors in the circuit are assumed by the following functions.

$$i_{rk}(v_k) = -g_1 v_k + g_3 v_k^3 \quad (g_1, g_3 > 0) \quad (1)$$

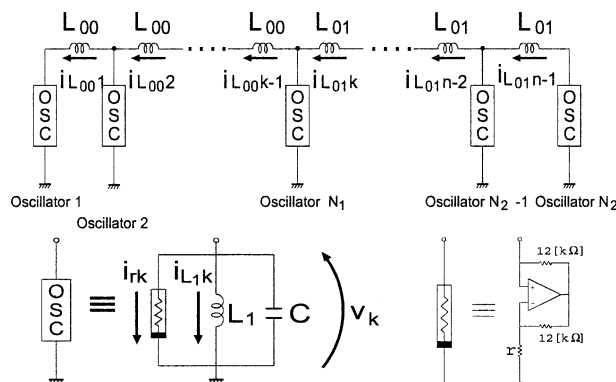


Fig. 1 Coupled van der Pol oscillators by two kinds inductors as a ladder.

Manuscript received December 19, 2003.

Manuscript revised March 27, 2004.

Final manuscript received May 17, 2004.

[†]The authors are with the Department of Electrical and Electronics Engineering, Faculty of Science and Technology, Sophia University, Tokyo, 102-8554 Japan.

^{††}The author is with the Department of Electrical and Electronic Engineering, Faculty of Engineering, University of Tokushima, Tokushima-shi, 770-8506 Japan.

^{†††}The author is with the Department of Mechanical-Electronic Engineering, Faculty of Engineering, Tokushima Bunri University, Sanuki-shi, 769-2193 Japan.

a) E-mail: yamauchi@ieee.org

The circuit equations governing the circuit in Fig. 1 are expressed as

[1st oscillator]

$$\begin{aligned} \dot{x}_1 &= y_1 \\ \dot{y}_1 &= -x_1 + \alpha_0(x_2 - x_1) + f(y_1) \end{aligned} \quad (2)$$

[2nd ~ ($N_1 - 1$)th oscillators]

$$\begin{aligned} \dot{x}_k &= y_k \\ \dot{y}_k &= -x_k + \alpha_0(x_{k+1} - 2x_k + x_{k-1}) + f(y_k) \end{aligned} \quad (3)$$

$(k = 2, 3, \dots, N_1 - 1)$

[N_1 th oscillator]

$$\begin{aligned} \dot{x}_{N_1} &= y_{N_1} \\ \dot{y}_{N_1} &= -x_{N_1} + \alpha_0(x_{N_1+1} - x_{N_1}) \\ &\quad + \alpha_1(x_{N_1-1} - x_{N_1}) + f(y_{N_1}) \end{aligned} \quad (4)$$

[($N_1 + 1$)th ~ ($N_2 - 1$)th oscillators]

$$\begin{aligned} \dot{x}_k &= y_k \\ \dot{y}_k &= -x_k + \alpha_1(x_{k+1} - 2x_k + x_{k-1}) + f(y_k) \end{aligned} \quad (5)$$

$(k = N_1+1, \dots, N_2 - 1)$

[N_2 th oscillator]

$$\begin{aligned} \dot{x}_{N_2} &= y_{N_2} \\ \dot{y}_{N_2} &= -x_{N_2} + \alpha_1(x_{N_2-1} - x_{N_2}) + f(y_{N_2}) \end{aligned} \quad (6)$$

where

$$f(y_k) = \varepsilon \left(y_k - \frac{1}{3} y_k^3 \right) \quad (7)$$

and

$$\begin{aligned} t &= \sqrt{L_1 C} \tau, \quad i_{L_1 k} = \sqrt{\frac{C g_1}{3 L_1 g_3}} x_k, \quad v_k = \sqrt{\frac{g_1}{3 g_3}} y_k, \\ \alpha_0 &= \frac{L_1}{L_{00}}, \quad \alpha_1 = \frac{L_1}{L_{01}}, \quad \varepsilon = g_1 \sqrt{\frac{L_1}{C}}, \quad \frac{d}{d\tau} = \text{“} \cdot \text{”}. \end{aligned} \quad (8)$$

The above variables and parameters are shown in Fig. 1. It should be noted that α_0 and α_1 correspond to the couplings and that ε corresponds to the nonlinearity. Equations (2)–(8) are calculated by using the fourth-order Runge-Kutta method with the stepsize $h = 0.001$.

3. Phase-Inversion Wave

In this section, we explain the phase-inversion waves observed from an array of van der Pol oscillators without discontinuity, which was investigated in [13]. Figure 2 shows an example of the phase-inversion waves.

In the computer calculations, we produced the phase-inversion waves as follows. Almost same initial conditions are given for all oscillators to produce complete in-phase synchronization, which is one of the steady states in the system. Next, invert the voltage and the current of one oscillator. In Fig. 2, a pair of phase-inversion waves is generated at the first oscillator.

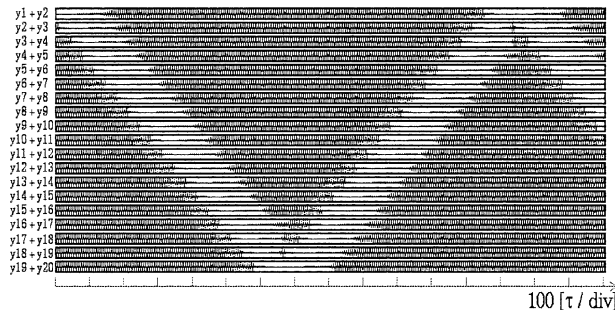


Fig. 2 Example of phase-inversion waves. $N_1 = N_2 = 20$, $\alpha_0 = 0.050$ and $\varepsilon = 0.20$.

In the diagrams, vertical axes are sums of voltages of adjacent oscillators and horizontal axis is time. Hence, black regions show phase states near in-phase synchronization, and white regions show phase states near anti-phase synchronization. We can observe the generation of a pair of phase-inversion waves, which is continuously existing wave propagation to change the phase states from in-phase to anti-phase and from anti-phase to in-phase.

4. Classification

In this section, we observe transmission and reflection of the phase-inversion waves for the case of $(N_1, N_2) = (11, 20)$. We fix the parameters $\varepsilon = 0.20$ and $\alpha_0 = 0.050$ and α_1 is varied as a control parameter. A pair of phase-inversion waves are generated at the first oscillator.

Figures 3 and 4 show the observed results. Figure 4 shows the phase differences between adjacent oscillators along time. Vertical axes are the phase differences between adjacent oscillators. Horizontal axes are time. $\Phi_{x,y}$ is a phase difference between x_{th} oscillator and y_{th} oscillator.

According to the parameter value of α_1 , the observed phenomena are classified into eight types as follows,

- (a) ~around 0.002: A pair of phase-inversion waves is reflected at the discontinuity almost completely.
- (b) around 0.003 ~ 0.025: A pair of phase-inversion waves is reflected and is transmitted. Complex phenomena are observed after the reflection and the transmission.
- (c) around 0.026 ~ 0.044: A pair of phase-inversion waves is reflected and is transmitted. The phase-inversion waves reflected at the discontinuity change to a pair of phase-waves.
- (d) around 0.045 ~ 0.054: A pair of phase-inversion waves is transmitted almost completely.
- (e) around 0.055 ~ 0.123: A pair of phase-inversion waves is transmitted. A new pair of phase-waves is generated after the phase-inversion waves are transmitted.
- (f) around 0.124 ~ 0.174: A pair of phase-inversion waves

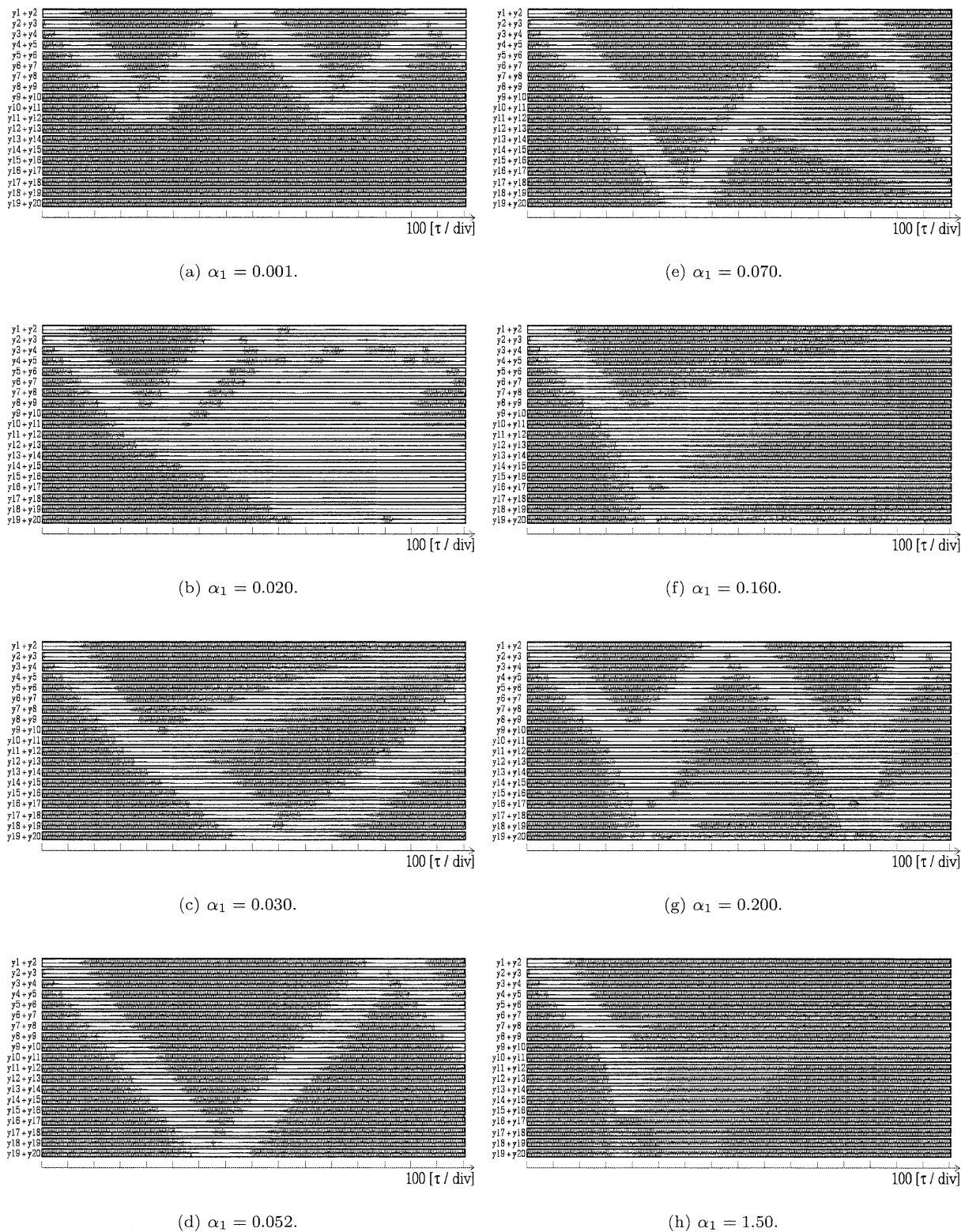


Fig. 3 Observation of the transmission and the reflection of a pair of phase-inversion waves. $N_1 = 11$, $N_2 = 20$, $\alpha_0 = 0.050$ and $\varepsilon = 0.20$.

is reflected and is transmitted. The phase-inversion waves change to phase-waves after the reflection and the transmission.

(g) around 0.175 ~ 0.232: A pair of phase-inversion waves is reflected and is transmitted. The phase-inversion

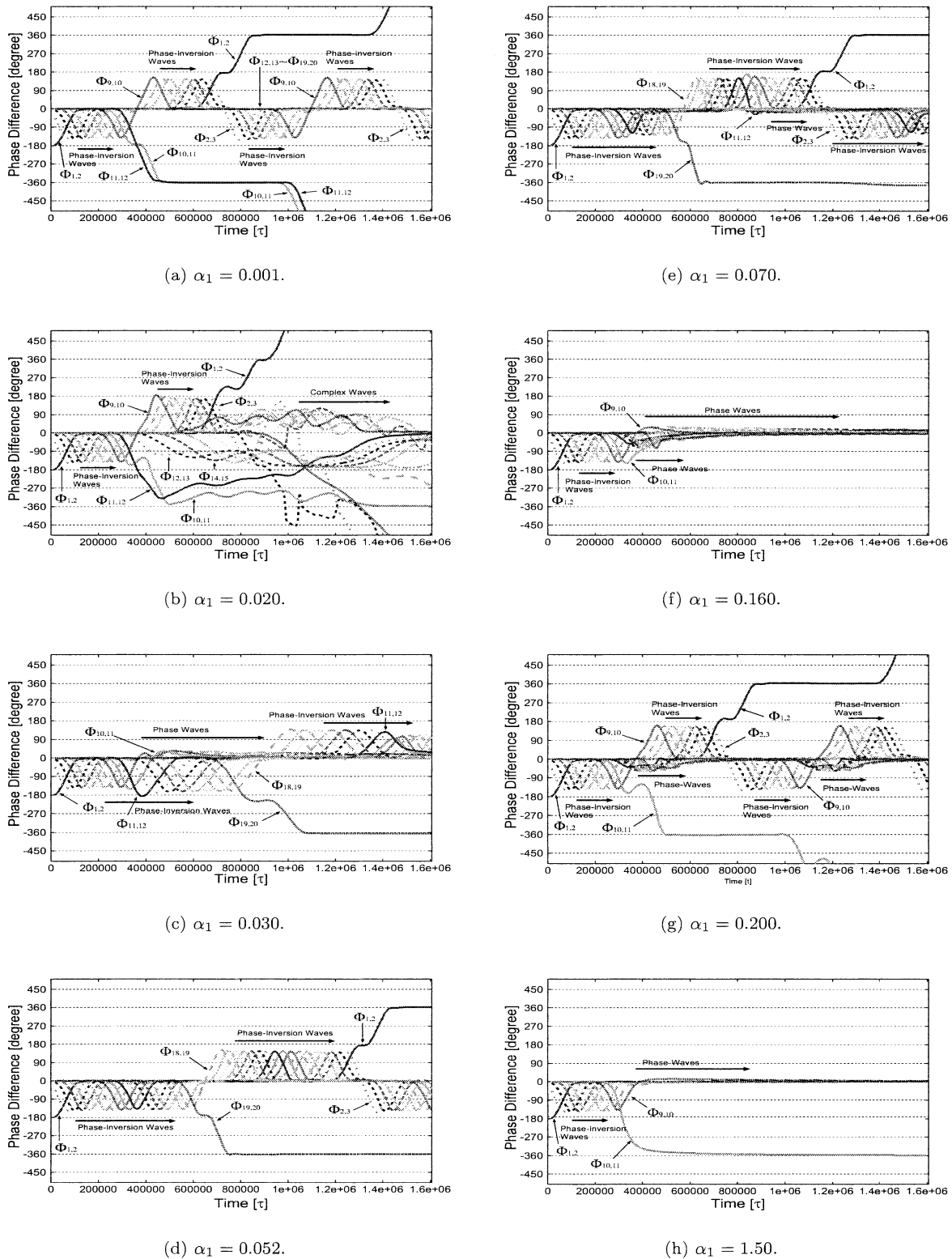


Fig. 4 Observation of the transmission and the reflection of a pair of phase-inversion waves by phase differences. $N_1 = 11, N_2 = 20, \alpha_0 = 0.050$ and $\varepsilon = 0.20$.

waves transmitted through the discontinuity change to a pair of phase-waves.

(h) around 0.233 ~: A pair of phase-inversion wave is reflected and is transmitted. The phase-inversion waves change to phase-waves after the transmission. It is

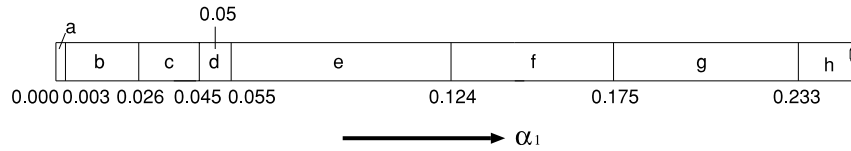


Fig. 5 Relationship between value of α_1 and observed phenomena. $N_1 = 11$, $N_2 = 20$, $\alpha_0 = 0.050$ and $\varepsilon = 0.20$.

difficult to observe in the figure, but the first phase-inversion wave is reflected at the discontinuity, collides with the second phase-inversion wave and changes to a pair of phase-waves.

It should be noted that we can observe different transmission phenomena for the cases of $L_{01} \gg L_{00}$ and $L_{01} < L_{00}$. Namely, for $L_{01} \gg L_{00}$ ($\alpha_1 \ll \alpha_0$), phase-inversion wave is not transmitted beyond the discontinuity. While, for $L_{01} < L_{00}$ ($\alpha_1 > \alpha_0$), phase-inversion wave is transmitted as phase-wave beyond the discontinuity. This interesting difference is explained in the Sect. 5.

Figure 5 summarizes the parameter regions corresponding to the above-mentioned eight types of the observed phenomena.

5. Mechanisms of Transmission and Reflection

In this section, the transmission mechanism and the reflection mechanism of the phase-inversion waves at the discontinuity are explained according to the computer calculated results in the previous section.

It has been already known that oscillation frequency of in-phase synchronization of oscillators coupled by inductors is different from that of anti-phase synchronization [5]. If we define the oscillation frequency of in-phase synchronization as f_{in} and the oscillation frequency of anti-phase synchronization as f_{anti} , f_{in} is smaller than f_{anti} [8]. Further, the difference between f_{in} and f_{anti} increases as coupling inductance increases. For example, when even van der Pol oscillators are coupled by inductors as a ring and ε is very small, theoretical values are obtained by Eqs. (9) and (10) [10].

[Frequency of in-phase synchronization]

$$f_{in} = \sqrt{\frac{1}{1+\alpha}} \cdot \frac{1}{2\pi} \quad (9)$$

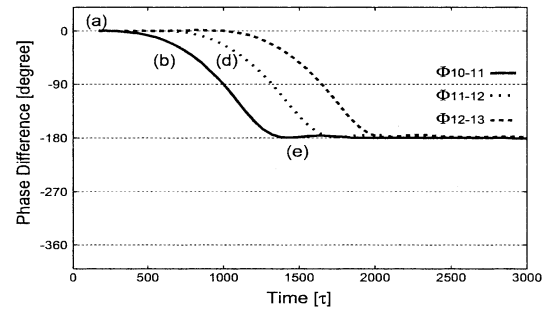
[Frequency of anti-phase synchronization]

$$f_{anti} = \sqrt{\frac{1+4\alpha}{1+\alpha}} \cdot \frac{1}{2\pi} \quad (10)$$

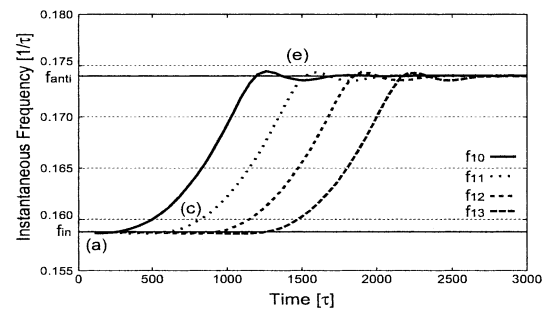
Computer calculated f_{in} and f_{anti} are slightly different from these values and are obtained by computer calculations as follows:

When $\alpha = 0.0500$ and $\varepsilon = 0.2000$, $f_{in} = 0.159$ [1/ τ] and $f_{anti} = 0.174$ [1/ τ].

We use this characteristic to explain the mechanisms



(a) Phase-difference.



(b) Instantaneous Frequency.

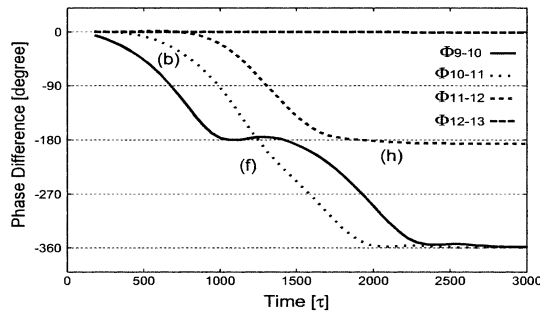
Fig. 6 Transmission at the discontinuity for the case of $\alpha_1 = \alpha_0$. $N_1 = 11$, $N_2 = 20$, $\alpha_0 = 0.0500$, $\alpha_1 = 0.0500$ and $\varepsilon = 0.20$.

of the transmission and the reflection of the phase-inversion waves. f_{in} and f_{anti} in Figs. 6, 7 and 8 show these values.

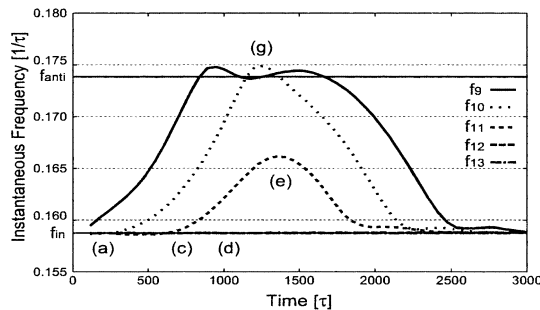
5.1 Transmission Mechanism

In order to explain the transmission mechanism, we consider the case of $\alpha_0 \approx \alpha_1$. Because the transmission is a typical phenomenon observed for that case. We can say the transmission mechanism is similar to the propagation mechanism [13] of a phase-inversion wave, if $\alpha_0 \approx \alpha_1$ is satisfied. Hence, the transmission mechanism is explained as follows:

1. Let us assume that OSC11 ~ OSC20 are in-phase synchronization and that the wave changing from in-phase into anti-phase is going to reach OSC11 from the direction of OSC1 (see (a) in Fig. 6).
2. As phase difference between OSC10 and OSC11 $\Phi_{10,11}$ approaches -180° (see (b) in Fig. 6), instantaneous frequency of OSC11 f_{11} changes from f_{in} to f_{anti} (see (c) in Fig. 6).



(a) Phase-difference.



(b) Instantaneous Frequency.

Fig. 7 Reflection at the discontinuity for the case of $\alpha_1 \ll \alpha_0$. $N_1 = 11$, $N_2 = 20$, $\alpha_0 = 0.0500$, $\alpha_1 = 0.0001$ and $\varepsilon = 0.20$.

3. The change of f_{11} causes decrease of $\Phi_{11,12}$ (see (d) in Fig. 6). Speed of the decrease is decided by the difference between f_{11} and f_{12} . This means that propagation speed of the wave is decided by the difference between f_{in} and f_{anti} .
4. When $\Phi_{11,12}$ reaches almost -180° , f_6 is equal to f_{anti} (see (e) in Fig. 6).

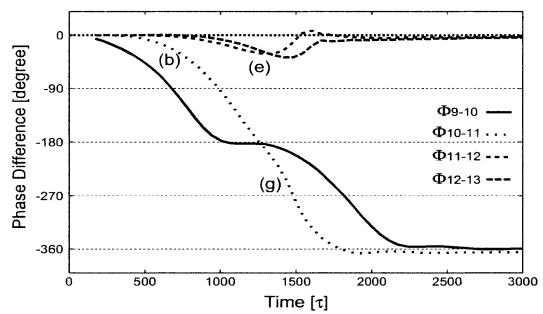
As a result, the phase-inversion wave is transmitted through the discontinuity.

5.2 Reflection Mechanism

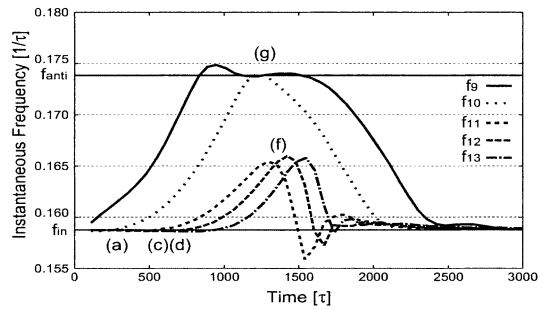
In order to explain the reflection mechanism, we consider two typical cases for the reflection. Namely the coupling parameter for one side of the discontinuity is much larger or much smaller than that of the other side.

5.2.1 When $L_{01} \gg L_{00}$ (i.e. $\alpha_1 \ll \alpha_0$)

1. Let us assume that OSC10~OSC20 are in-phase synchronization and that a phase-inversion wave from in-phase to anti-phase reaches at OSC10 from the direction of OSC1.
2. Instantaneous frequency of OSC10 f_{10} begins to



(a) Phase-difference.



(b) Instantaneous Frequency.

Fig. 8 Reflection at the discontinuity for the case of $\alpha_1 \gg \alpha_0$. $N_1 = 11$, $N_2 = 20$, $\alpha_0 = 0.0500$, $\alpha_1 = 0.2000$ and $\varepsilon = 0.20$.

change from f_{in} toward f_{anti} , because in-phase synchronization between OSC9 and OSC10 breaks by the phase-inversion wave (see (a) in Fig. 7).

3. As f_{10} changes from f_{in} to f_{anti} , phase difference between OSC10 and OSC11 $\Phi_{10,11}$ approaches -180° (see (b) in Fig. 7).
4. As $\Phi_{10,11}$ approaches -180° , f_{11} begins to change from f_{in} to f_{anti} (see (c) in Fig. 7).
5. Change of f_{11} does not propagate to OSC12 immediately, because L_{01} is much larger than L_{00} (see (d) in Fig. 7).
6. Hence, f_{11} cannot reach f_{anti} and begins returning to f_{in} (see (e) in Fig. 7).
7. As f_{11} returns to f_{in} , $\Phi_{10,11}$ continues to increase until reaching -360° (see (f) in Fig. 7).
8. By the effect of the decrease of $\Phi_{10,11}$, f_{10} begins to decrease again from f_{anti} toward f_{in} (see (g) in Fig. 7).
9. $\Phi_{11,12}$ becomes -180° , because in spite of constant value which is f_{12} , f_{11} changes from f_{anti} and returns to f_{in} again (see (h) in Fig. 7).

Remark: As L_{01} approaches L_{00} , it becomes easier that change of f_{11} propagates to OSC12. Hence, we could observe that the phase-inversion wave is transmitted beyond the discontinuity as shown in Figs. 2(b), (c) and 3(b), (c). On the other hand, the reflection becomes smaller, because being hard to change f_{11} is the main reason of the generation of the reflection.

5.2.2 When $L_{01} \ll L_{00}$ (i.e. $\alpha_1 \gg \alpha_0$)

1. Let us assume that OSC10~OSC20 are in-phase synchronization and that a wave from in-phase to anti-phase reaches at OSC10 from the direction of OSC1.
2. Instantaneous frequency of OSC10 f_{10} begins to change from f_{in} toward f_{anti} , because in-phase synchronization between OSC9 and OSC10 breaks by the phase-inversion wave (see (a) in Fig. 8).
3. As f_{10} changes from f_{in} to f_{anti} , phase difference between OSC10 and OSC11 $\Phi_{10,11}$ approaches -180° (see (b) in Fig. 8).
4. As $\Phi_{10,11}$ approaches -180° , f_{11} changes from f_{in} to f_{anti} (see (c) in Fig. 8).
5. Change of f_{11} propagates to OSC12 immediately, because L_{01} is much smaller than L_{00} (see (d) in Fig. 7).
6. Hence, in-phase synchronization between OSC11 and OSC12 is hard to break (see (e) in Fig. 8). And f_{11} and f_{12} return to f_{in} together (see (f) in Fig. 8).
7. As f_{11} returns to f_{in} , $\Phi_{10,11}$ continues to increase until reaching -360° (see (g) in Fig. 8).

Hence, when L_{01} is much smaller than L_{00} , the transmission always exists with the reflection.

Remark: As L_{01} approaches L_{00} , it becomes more difficult that phase states of OSC11 and OSC12 hold in-phase synchronization. Hence, the reflection of the phase-inversion wave disappears as shown in Figs. 2(d), (e) and 3(d), (e).

6. Circuit Experiments

In this section, we confirm the generation of the transmission and the reflection of the phase-inversion wave by circuit experiments. The typical result for $(N_1, N_2) = (7, 10)$ is shown in Fig. 9. The corresponding computer simulated result is shown in Fig. 10. We observe that the circuit experimental result and the computer simulated result agree well. The small amount of the difference between the two results may come from the resistance in real inductors or difficulty of setting initial phase difference in real circuit experiments.

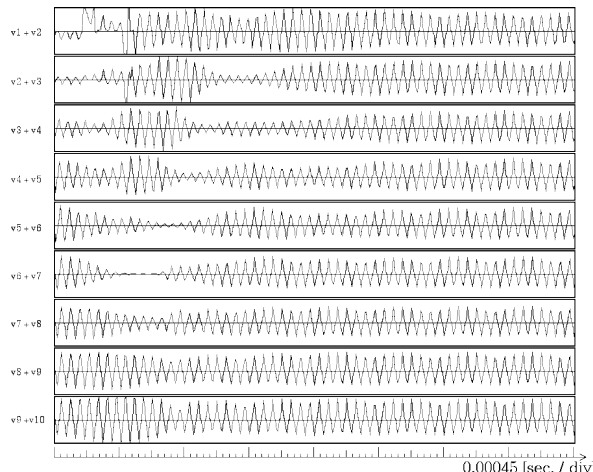


Fig. 9 Experimental result. $N_1 = 7, N_2 = 10, L_{00} = 1160$ [mH], $L_{01} = 242$ [mH], $L_1 = 200$ [mH], $C = 47$ [nF] and $r = 1$ [k Ω].

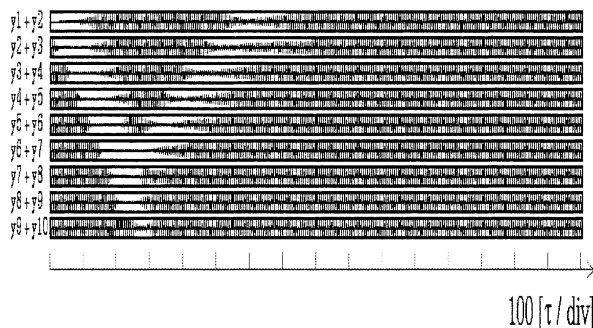


Fig. 10 Computer simulated result. $N_1 = 7, N_2 = 10, \alpha_0 = 0.0500, \alpha_1 = 0.2800$ and $\varepsilon = 0.20$.

7. Conclusions

In this study, we observed behavior of a pair of phase-inversion waves around the discontinuity of the system consisting of two parts of coupled van der Pol oscillators. Observed phenomena by computer calculations were classified into eight types. We explained the mechanism of the transmission and the reflection of the phase-inversion wave at the discontinuity and made clear that different mechanisms reflect the waves for the cases of $L_{01} > L_{00}$ and $L_{01} < L_{00}$. Further, we observed a pair of phase-inversion waves by circuit experiments. The circuit experimental results agreed with the numerical calculated results very well.

References

- [1] L.L. Bonilla, C.J. Pérez Vicente, and R. Spigler, "Time-periodic phases in populations of nonlinearly coupled oscillators with bimodal frequency distributions," *Physica D: Nonlinear Phenomena*, vol.113, no.1, pp.79–97, Feb. 1998.
- [2] J.A. Sherratt, "Invading wave fronts and their oscillatory wakes are linked by a modulated traveling phase resetting wave," *Physica D: Nonlinear Phenomena*, vol.117, no.1-4, pp.145–166, June 1998.
- [3] G. Abramson, V.M. Kenkre, and A.R. Bishop, "Analytic solutions

for nonlinear waves in coupled reacting systems," *Physica A: Statistical Mechanics and its Applications*, vol.305, no.3-4, pp.427-436, March 2002.

- [4] C.M. Gray, "Synchronous oscillations in neuronal systems: Mechanisms and functions," *J. Comput. Neurosci.*, vol.1, pp.11-38, 1994.
- [5] T. Suezaki and S. Mori, "Mutual synchronization of two oscillators," *Trans. IECE*, vol.48, no.9, pp.1551-1557, Sept. 1965.
- [6] A.C. Scott, "Distributed multimode oscillators of one and two spatial dimensions," *IEEE Trans. Circuit Theory*, vol.CT-17, no.1, pp.55-60, Feb. 1970.
- [7] D.A. Linkens, "Analytical solution of large numbers of mutually coupled nearly sinusoidal oscillators," *IEEE Trans. Circuits Syst.*, vol.CAS-21, no.2, pp.294-300, March 1974.
- [8] T. Endo and S. Mori, "Mode analysis of a multimode ladder oscillator," *IEEE Trans. Circuits Syst.*, vol.CAS-23, no.2, pp.100-113, Feb. 1976.
- [9] T. Endo and S. Mori, "Mode analysis of two-dimensional low-pass multimode oscillator," *IEEE Trans. Circuits Syst.*, vol.CAS-23, no.9, pp.517-530, Sept. 1976.
- [10] T. Endo and S. Mori, "Mode analysis of a ring of a large number of mutually coupled van der Pol oscillators," *IEEE Trans. Circuits Syst.*, vol.CAS-25, no.1, pp.7-18, Jan. 1978.
- [11] S.P. Datarina and D.A. Linkens, "Multimode oscillations in mutually coupled van der Pol type oscillators with fifth-power nonlinear characteristics," *IEEE Trans. Circuits Syst.*, vol.CAS-25, no.1, pp.308-315, May 1978.
- [12] S. Moro, Y. Nishio, and S. Mori, "Synchronization phenomena in oscillators coupled by one resistor," *IEICE Trans. Fundamentals*, vol.E78-A, no.2, pp.244-253, Feb. 1995.
- [13] M. Yamauchi, M. Wada, Y. Nishio, and A. Ushida, "Wave propagation phenomena of phase states in oscillators coupled by inductors as a ladder," *IEICE Trans. Fundamentals*, vol.E82-A, no.11, pp.2592-2598, Nov. 1999.
- [14] M. Yamauchi, Y. Nishio, and A. Ushida, "Phase-waves in a ladder of oscillators," *IEICE Trans. Fundamentals*, vol.E86-A, no.4, pp.891-899, April 2003.



Masayuki Yamauchi received the B.E., M.E. and Ph.D. degrees from University of Tokushima, Tokushima, Japan, in 1998, 2000 and 2003, respectively. In 2003, he joined the Department of Electrical and Electronics Engineering at Sophia University, Tokyo, Japan, where he is currently an Assistant Professor. His research interests include analysis of nonlinear phenomena in coupled oscillators and development of applications of data mining. Dr. Yamauchi is a member of the IEEE.



Yoshifumi Nishio received the B.E., M.E. and Ph.D. degrees in Electrical Engineering from Keio University, Yokohama, Japan, in 1988, 1990 and 1993, respectively. In 1993, he joined the Department of Electrical and Electronic Engineering at University of Tokushima, Tokushima, Japan, where he is currently an Associate Professor. From May 2000 he spent a year in the Laboratory of Nonlinear Systems (LANOS) at the Swiss Federal Institute of Technology Lausanne (EPFL) as a visiting professor.

His research interests include analysis and application of chaos in electrical circuits, analysis of synchronization in nonlinear circuits, development of analytical methods for nonlinear circuits and theory and application of cellular neural networks. Dr. Nishio is a member of the IEEE.



Akio Ushida received the B.E. and M.E. degrees in Electrical Engineering from University of Tokushima in 1961 and 1966, respectively, and the Ph.D. degree in Electrical Engineering from University of Osaka Prefecture in 1974. He was an Associate Professor from 1973 to 1980 at University of Tokushima. From 1980 to 2003 he had been a Professor in the Department of Electrical and Electronic Engineering at University of Tokushima. Since 2003 he has been a Professor in the Department of Mechanical-

Electronic Engineering, Faculty of Engineering, Tokushima Bunri University. From 1974 to 1975 he spent one year as a visiting scholar at the Department of Electrical Engineering and Computer Sciences at the University of California, Berkeley. His current research interests include numerical methods and computer-aided analysis of nonlinear systems. Dr. Ushida is a member of IEEE.



Mamoru Tanaka received the B.E., M.E. and Ph.D. degrees in Electrical Engineering from Keio University, Yokohama, Japan, in 1972, 1974 and 1981, respectively. In 1974, he joined the Circuit Development Department, Computer Engineering Division, Nippon Electric Company (NEC) where he was engaged in design and development of NEC's LSI computers. He resigned from the company and entered graduate school at Keio University in 1978. In April 1981, he became an Associate Professor

in the Department of Electrical and Electronics Engineering at Sophia University, Tokyo, Japan. He is now a Professor at Sophia University. He has undertaken research on the analysis of large-scale networks, architectures of new LSI computers and data mining. Dr. Tanaka was an Associate Editor of the IEEE Transactions on Circuits and Systems.